

# Pressure Masks for Point-like Contact with Elastic Models

Doug L. James<sup>1</sup> and Dinesh K. Pai<sup>1,2</sup>

University of British Columbia

## Abstract

In this paper, we introduce pressure masks for supporting the convenient abstraction of localized scale-specific point-like contact with a discrete elastic object. While these masks may be defined for any elastic model, special attention is given to the case of point-like contact with precomputed linear elastostatic models for purposes of haptic force-feedback.

## 1 Introduction

It has long been recognized that point contact is a convenient abstraction for haptic interactions, and the PHANToM™ haptic interface is a testament to that fact. While it is possible to consider the contact area to be truly a point for rigid models, this is not possible for elastic models, as infinite contact pressure can lead to various inconsistencies. The solution is simply to assume the contact zone has tractions distributed over a finite surface area. We propose to do this efficiently and consistently by introducing *pressure masks* for defining nodal traction distributions. This addresses at least two core issues. First, having a point contact with force distributed over a finite area is somewhat contradictory, and the traction distribution is effectively an underdetermined quantity without any inherent spatial scale. This is resolved by treating the contact as a single displacement constraint whose traction distribution enters as a user (or manipulandum) specified parameter. The distribution of force on the surface of the model can then be consistently specified in a fashion which is independent of the scale of the mesh. Second, given the model is discrete, special care must be taken to ensure a sufficiently regular force response on the surface, since irregularities are very noticeable during sliding contact motions. By suitably interpolating nodal force responses, displacement constraints can be imposed which will result in regular haptic force-feedback.

The pressure mask approach is particularly effective for haptics when used with linear elastostatic models with precomputed Green's functions, since force response can usually be computed at  $\mathcal{O}(1)$  cost. In §2, minimal definitions and notation for discussing the elastostatic model are presented. Afterwards, in §3, the construction and definition of pressure masks is given, and it is shown how to compute nodal (or vertex) stiff-

nesses for elastostatic models and then use these to consistently define the surface's stiffness.

Much of this material is presented in much greater detail in [JP]; throughout, an identical notation is used.

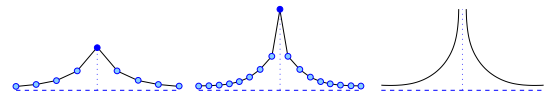


Figure 1: *Point Contact Must Not be Taken Literally for Elastic Models* : This figure illustrates the development of a displacement singularity associated with a concentrated surface force as the continuum limit is approached. In the left image, a unit force applied to a vertex of a discrete elastic model results in a finite vertex displacement. As the model's mesh is refined (middle and right image), the same concentrated force load eventually tends to produce a singular displacement at the contact location, and the stiffness of any single vertex approaches zero (see Table 6).

## 2 Linear Elastostatic Model Background

Precomputed linear elastostatic models of various discretization origins are efficient candidates for real time haptic interaction [BC96, JP99, JP]. A general boundary Green's function description is now very briefly presented for use in §3.

### 2.1 Nodal Displacement and Traction Variables

Consider a discrete elastic model with  $n$  surface nodes, e.g., polyhedral mesh vertices, for which nodal quantities are defined. Specifically, let the surface displacement  $\mathbf{u}(\mathbf{x})$  and traction  $\mathbf{p}(\mathbf{x})$  fields be parametrized by  $n$ -vectors of nodal variables,

$$\mathbf{u} = [\mathbf{u}_1, \dots, \mathbf{u}_n]^T \quad (1)$$

$$\mathbf{p} = [\mathbf{p}_1, \dots, \mathbf{p}_n]^T, \quad (2)$$

where each of the values  $\mathbf{u}_k$  and  $\mathbf{p}_k$  belong to  $\mathbb{R}^3$ . Since our boundary element implementation uses vertex-based triangle mesh models, we shall often refer to a node as a vertex.

<sup>1</sup>Institute of Applied Mathematics

<sup>2</sup>Dept. of Computer Science, {djames|pai}@cs.ubc.ca

## 2.2 Reference Boundary Value Problem (RBVP) Definition

A major benefit of using linear elastostatic models for haptics is that it is possible to precompute the Green's functions to one particular class of boundary value problem (BVP), a relevant *reference BVP* (RBVP), and be able to efficiently compute components of those solutions rapidly at run time (see Figure 2).

Without loss of generality, assume that either position or traction constraints are specified at each boundary node. Let the mutually exclusive nodal index sets  $\Lambda_u^0$  and  $\Lambda_p^0$  specify nodes with displacement and traction constraints, respectively, so that  $\Lambda_u^0 \cap \Lambda_p^0 = \emptyset$  and  $\Lambda_u^0 \cup \Lambda_p^0 = \{1, 2, \dots, n\}$ . Specifying boundary values at each of the  $n$  nodes defines a BVP to be solved for desired unknown variables, e.g., haptic contact forces, at each step of the simulation. Denote the unspecified and complementary specified nodal variables by

$$v_j = \begin{cases} p_j & : j \in \Lambda_u^0 \\ u_j & : j \in \Lambda_p^0 \end{cases} \quad \text{and} \quad \bar{v}_j = \begin{cases} \bar{u}_j & : j \in \Lambda_u^0 \\ \bar{p}_j & : j \in \Lambda_p^0 \end{cases} \quad (3)$$

respectively.

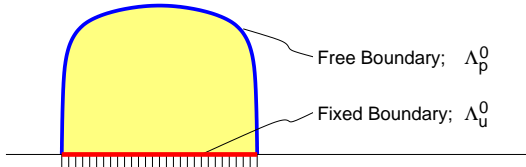


Figure 2: *Reference Boundary Value Problem (RBVP) Example:* The RBVP associated with a model attached to a rigid support is shown with boundary regions having fixed ( $\Lambda_u^0$ ) or free ( $\Lambda_p^0$ ) nodal constraints indicated. A typical haptic simulation would then impose contacts on the free boundary nodes,  $\Lambda_p^0$ .

## 2.3 RBVP Solution using Green's Functions

The general solution of the RBVP is conveniently expressed using Green's functions of the RBVP as

$$v = \Xi \bar{v} = \sum_{j \in \Lambda_u^0} \xi_j \bar{u}_j + \sum_{j \in \Lambda_p^0} \xi_j \bar{p}_j, \quad (4)$$

where the *reference system Green's functions* (RSGFs) are the block columns of the matrix

$$\Xi = [\xi_1 \xi_2 \cdots \xi_n] \in \mathbb{R}^{3n \times 3n}. \quad (5)$$

The  $j^{th}$  RSGF describes the effect of the  $j^{th}$  node's specified boundary value,  $\bar{v}_j$ . In practice it is only necessary to compute RSGFs for nodes which may have changing nonzero boundary values during the simulation.

Since the RSGFs only depend on the RBVP and the geometric and material properties of the deformable object, they may be precomputed for use in a simulation.

Note that this applies to any discrete linear elastostatic model, regardless of internal material properties or the discretization technique employed.

## 3 Surface Stiffness Models for Point-like Contact

This section presents the pressure mask approach for elastic models (§3.1), then specializes to linear elastostatic models for which the pressure masks may be used to compute vertex stiffnesses (§3.2) which are in turn used to compute the surface stiffness (§3.3).

### 3.1 Pressure Masks for Distributed Point-like Contacts

In this section, pressure masks are defined and used to specify the traction distribution associated with force applied via a masked vertex constraint.

#### 3.1.1 Discrete Traction Space Definitions

In order to characterize traction distributions for the discussion of mask construction and the smoothness of force response, it is necessary to define a discrete scalar function space,  $\mathcal{L}$ , on the model's boundary,  $\Gamma$ . Let

$$\mathcal{L} = \text{span} \{ \phi_j(\mathbf{x}), \quad j = 1 \dots n, \quad \mathbf{x} \in \Gamma \}, \quad (6)$$

where  $\phi_j(\mathbf{x})$  is a scalar basis function associated with the  $j^{th}$  node. The traction field is then a vector function whose components lie in  $\mathcal{L}$ ,

$$\mathbf{p} = \mathbf{p}(\mathbf{x}) = \sum_{j=1}^n \phi_j(\mathbf{x}) \mathbf{p}_j.$$

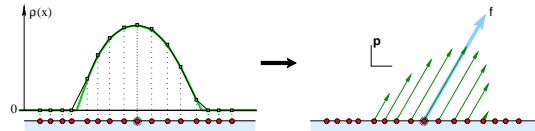


Figure 3: *Collocated Scalar Masks:* A direct means for obtaining a relative pressure amplitude distribution about each node, is to employ a user-specified scalar functional of the desired spatial scale. The scalar pressure mask is then given by nodal collocation (left), after which the vector traction distribution associated with a nodal point load is then computed as the product of the applied force vector and the (compactly supported) scalar mask (right).

#### 3.1.2 Pressure Mask Definition

Scalar relative pressure masks provide a flexible means for modeling vector pressure distributions associated with each node. This allows a force applied at the  $i^{th}$

node to generate a traction distribution which is a linear combination of  $\{\phi_j(\mathbf{x})\}$  and not just  $\phi_i(\mathbf{x})$ .

In the continuous setting, a scalar surface density  $\rho(\mathbf{x}) : \Gamma \rightarrow \mathbb{R}$  will relate the localized contact force  $\mathbf{f}$  to the applied traction  $\mathbf{p}$  via

$$\mathbf{p}(\mathbf{x}) = \rho(\mathbf{x})\mathbf{f}$$

which in turn implies the normalization condition

$$\int_{\Gamma} \rho(\mathbf{x}) d\Gamma \mathbf{x} = 1. \quad (7)$$

In the discrete setting, the surface density on  $\Gamma$  is

$$\rho(\mathbf{x}) = \sum_{j=1}^n \phi_j(\mathbf{x}) \rho_j \in \mathcal{L}, \quad (8)$$

and is parameterized by scalar pressure mask vector,

$$\rho = [\rho_1, \rho_2, \dots, \rho_n]^T.$$

Substituting (8) into (7), the discrete normalization condition satisfied becomes

$$a^T \rho = 1, \quad (9)$$

where

$$a_i = \int_{\Gamma} \phi_i(\mathbf{x}) d\Gamma \mathbf{x} \quad (10)$$

defines the *vertex area*. Notice that the mask density  $\rho$  has units of  $\frac{1}{\text{area}}$ .

In practice, the vertex pressure mask  $\rho$  may be specified in a variety of ways. It could be specified at runtime, e.g., as the byproduct of a physical contact mechanics solution, or be a user specified quantity. We shall consider the case where there is a compactly supported scalar function  $\rho(\mathbf{x})$  specified at each vertex on the free boundary. The corresponding pressure mask  $\rho$  may then be defined using nodal collocation (see Figure 3),

$$\rho_j = \begin{cases} \rho(\mathbf{x}_j), & j \in \Lambda_p^0, \\ 0, & j \in \Lambda_p^0, \end{cases},$$

followed by suitable normalization to satisfy (9).

In the following, denote the density mask for the  $i^{th}$  vertex by the  $n$ -vector  $\rho^i$ , with nonzero values being indicated by the set of masked nodal indices  $\mathcal{M}_i$ . Since the intention is to distribute force on the free boundary, masks will only be defined for  $i \in \Lambda_p^0$ . Additionally, these masks will only involve nodes on the free boundary,  $\mathcal{M}_i \subset \Lambda_p^0$ , as well as be nonempty,  $|\mathcal{M}_i| > 0$ .

### 3.1.3 Example: Spherical Mask Functionals

Spherically symmetric mask functionals with a scale parameter were suitable candidates for constructing vertex masks via collocation on smooth surfaces. One example, which was commonly used (see Figure 4 and 6), is a functional with linear radial dependence,

$$\rho^i(\mathbf{x}; r) = \begin{cases} 1 - \frac{|\mathbf{x} - \mathbf{x}_i|}{r}, & |\mathbf{x} - \mathbf{x}_i| < r, \\ 0, & \text{otherwise.} \end{cases},$$

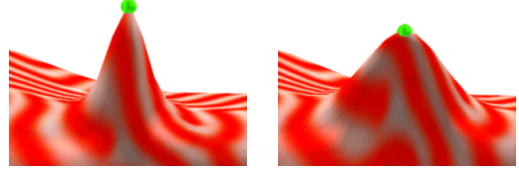


Figure 4: *Illustration of Changing Mask Scale:* Exaggerated pulling deformations clearly illustrate different spatial scales in the underlying traction distribution. In each case, pressure masks were automatically generated using the linear spherical mask functional (see §3.1.3) for different values of the radius parameter,  $r$ . This example shows (left) a single vertex mask, and (right) a mask involving several nearby vertices. Note that in each case the surface has been once refined using Loop subdivision.

where  $r$  specifies the radial scale<sup>1</sup>. The effect of changing  $r$  is shown in Figure 4.

## 3.2 Vertex Stiffnesses using Pressure Masks

Having consistently characterized point-like force loads using vertex pressure masks, it is now possible to calculate the stiffness of each vertex. In the following sections, these vertex stiffnesses will then be used to compute the stiffness at any point on model's surface for haptic rendering of point-like contact.

### 3.2.1 Elastic Vertex Stiffness

For any single node,  $i$ , on the free,  $i \in \Lambda_p^0$ , or rigidly fixed boundary,  $i \in \Lambda_u^0$ , a finite force stiffness,  $\mathbf{K}_i \in \mathbb{R}^{3 \times 3}$ , may be associated with its displacement, i.e.,

$$\mathbf{f} = \mathbf{K}_i \mathbf{u}_i, \quad i \in \Lambda_p^0.$$

Given a force  $\mathbf{f}$  applied at vertex  $i \in \Lambda_p^0$ , the corresponding distributed traction constraints are

$$\mathbf{p}_j = \rho_j^i \mathbf{f}. \quad (11)$$

Then using (4), the displacement of the  $i^{th}$  vertex is

$$\mathbf{u}_i = \sum_{j \in \mathcal{M}_i} \Xi_{ij} \mathbf{p}_j = \sum_{j \in \mathcal{M}_i} \rho_j^i \Xi_{ij} \mathbf{f},$$

so that the effective stiffness of the masked vertex is

$$\mathbf{K}_i = \left( \sum_{j \in \mathcal{M}_i} \rho_j^i \Xi_{ij} \right)^{-1}, \quad i \in \Lambda_p^0. \quad (12)$$

It follows from (4) and (11) that the corresponding globally consistent solution is

$$\mathbf{v} = \zeta_i \mathbf{f} = \left( \sum_{j \in \mathcal{M}_i} \rho_j^i \xi_j \right) \mathbf{f} \quad (13)$$

<sup>1</sup> $r$  may be thought of as the size of the haptic probe's tip.

where  $\zeta_i$  is the convolution of the RSGFs with the mask  $\rho^i$ , and characterizes the distributed force load.

# Vertices	Single $\ \mathbf{K}\ _2$	Masked $\ \mathbf{K}\ _2$
34	7.3	13.3
130	2.8	11.8
514	1.1	11.2

Figure 5: *Vertex Stiffness Dependence on Mesh Resolution:* This table shows vertex stiffness magnitudes (arbitrary units) for a BEM model at three different Loop subdivision mesh resolutions. The stiffness corresponding to a single vertex constraint exhibits a large dependence on mesh resolution, and has a magnitude which rapidly decreases to zero as the mesh is refined. On the other hand, the stiffness generated using a vertex pressure mask (collocated linear sphere functional (see §3.1.3) with radius equal to the coarsest mesh’s mean edge length) has substantially less mesh dependence, and quickly approaches a nonzero value.

### 3.2.2 Rigid Vertex Stiffness

For surfaces of rigid models, a finite force response may be defined using an isotropic stiffness matrix,

$$\mathbf{K}^R = k^{\text{Rigid}} \mathbf{I}_3 \in \mathbb{R}^{3 \times 3}, \quad k^{\text{Rigid}} \in \mathbb{R}.$$

This is useful for defining a response at position constrained vertices of a deformable model,

$$\mathbf{K}_j = \mathbf{K}^R, \quad j \in \Lambda_u^0, \quad (14)$$

for determining contact responses on neighbouring triangles which are not rigid.

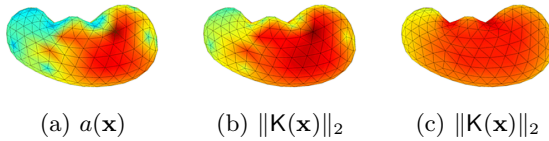


Figure 6: *Effect of Pressure Masks on Surface Stiffness:* Even models with reasonable mesh quality, such as this simple BEM kidney model, can exhibit haptically perceptible surface stiffness irregularities when single-vertex stiffnesses are used. A plot (a) of the vertex area,  $a$ , clearly indicates regions of large (dark red) and small (light blue) triangles. In (b) the norm of the single-vertex surface stiffness,  $\|\mathbf{K}(\mathbf{x})\|_2$ , reveals a noticeable degree of mesh-related stiffness artifacts. On the other hand, the stiffness plotted in (c) was generated using a pressure mask (collocated linear sphere functional (see §3.1.3) of radius twice the mesh’s mean edge length) and better approximates the regular force response expected of such a model.

### 3.3 Surface Stiffness from Vertex Stiffnesses

Given the vertex stiffnesses,  $\{\mathbf{K}_j\}_{j=1}^n$ , the surface stiffness is defined using nodal interpolation

$$\mathbf{K}(\mathbf{x}) = \sum_{j=1}^n \phi_j(\mathbf{x}) \mathbf{K}_j, \quad \mathbf{x} \in \Gamma, \quad (15)$$

so that  $(\mathbf{K}(\mathbf{x}))_{ij} \in \mathcal{L}$ . Note that there are usually only a small number of nonzero terms in the sum of (15). In this way, the surface stiffness may be continuously defined using only  $|\Lambda_p^0|$  free boundary vertex stiffnesses and a single rigid stiffness parameter,  $k^{\text{Rigid}}$ , regardless of the extent of the masks. The benefit of pressure masks is clearly visible in Figure 6 for piecewise linear  $\mathcal{L}$ .

It follows [JP] that the global deformation corresponding to the displacement constraint  $\bar{\mathbf{u}}$  applied on the free boundary at  $\mathbf{x} \in \Gamma$  is

$$\mathbf{v} = \sum_{i \in \Lambda_p^0} \zeta_i \phi_i(\mathbf{x}) \mathbf{f} = \sum_{i \in \Lambda_p^0} \left( \sum_{j \in \mathcal{M}_i} \rho_j^i \xi_j \right) \phi_i(\mathbf{x}) \mathbf{f}. \quad (16)$$

We note that this may be interpreted as an elastostatic generalization of force shading [MS96].

## 4 Summary and Conclusion

We have introduced pressure masks for the consistent definition of forces arising from point-like haptic interactions. This leads to a computationally efficient means for obtaining regular surface force responses from discrete elastostatic models. Experiments using a PHANToM™ interface confirmed that the pressure masks produced a perceptible improvement.

## References

- [BC96] Morten Bro-Nielsen and Stephane Cotin. Real-time volumetric deformable models for surgery simulation using finite elements and condensation. *Computer Graphics Forum*, 15(3):57–66, August 1996.
- [JP] Doug L. James and Dinesh K. Pai. A unified treatment of elastostatic and rigid contact simulation for real time haptics. To appear.
- [JP99] Doug L. James and Dinesh K. Pai. Art-Defo: Accurate Real Time Deformable Objects. *Computer Graphics*, 33(Annual Conference Series):65–72, 1999.
- [MS96] Hugh B. Morgenbesser and Mandayam A. Srinivasan. Force shading for haptic shape perception. In *Proceedings of the ASME Dynamics Systems and Control Division*, volume 58, 1996.